

Reconstruction of Anorganic Mammalian Bone by Surface-Initiated Polymerization of L-Lactide

Troy Wiegand,[†] Jeremy Karr,[‡] Jay D. Steinkruger,[§] Kris Hiebner,[†] Bobby Simetich,^{||} Mark Beatty,^{||} and Jody Redepenning^{*,†}

Department of Chemistry, University of Nebraska, Lincoln, Nebraska 68588 and College of Dentistry, University of Nebraska Medical Center, Lincoln, Nebraska 68583

Received March 28, 2008. Revised Manuscript Received May 24, 2008

Polymerization of L-lactide within the pores of anorganic mammalian bone is described. No additional solvent or catalyst is used. The resulting composites exhibit macroscopic morphologies and mechanical properties similar to that of the original bone. We observe an average compressive strength of 194 MPa and an elastic modulus of 8.8 GPa for composites comprised of poly-L-lactide and anorganic bone derived from bovine femurs. Modeling of the reaction kinetics with synthetic sources of crystalline hydroxyapatite powder suggests that polymerization proceeds via a surface-initiated mechanism that is first order in surface area of hydroxyapatite and first order in mole fraction of L-lactide.

Introduction

Challenges to materials science and medicine regarding hard tissue replacement have existed for at least 3000 years. Archeological records from the early Bronze Age demonstrate that attempts were made, probably unsuccessfully, to repair trephinated human skulls with autografts.¹ By 600 A.D. the Mayan civilization used seashell nacre with some success for dental implants.² Shortly after Hulagu Khan led the 1258 A.D. Mongol invasion of Baghdad, Zakaria al-Qazwini, an Arab scientist and cosmographer, documented problematic tissue rejection associated with transplantation of interspecies mammalian bone tissue into humans. He also noted the superior performance of porcine bone as a viable source of bone tissue when a human source was not available.³ In present day Iraq, the medical response to traumatized bone remains an important issue. Soldiers in ongoing armed conflicts are experiencing high rates of orthopedic trauma, such as segmental bone defects, caused by improvised explosive devices (IEDs).⁴ The need for improved orthopedic biomaterials is no less relevant to the civilian population. As baby boomers approach retirement age, there is an increasing need to repair and restore their damaged bones and tissues. As individuals age, their musculoskeletal support structures lose resilience in response to

trauma. Additionally, inherited disorders and disease can cause life-changing or life-threatening damage to the skeletal system.

Significant challenges confront materials scientists and physicians interested in viable sources of materials for tissue repair and replacement.^{5,6} Tissues for allografts, where the donor and recipient are the same species, are frequently in short supply. For some applications, xenogeneic tissues are a viable alternative to human sources of materials; however, immunological barriers prevent routine transplantation of tissue from one species to another.⁷ The use of tissues from species genetically similar to humans is desirable to lessen the severity of rejection. Unfortunately, tissues from these species pose a threat because of the higher likelihood of pathogens or infectious disease being transmitted to the recipient.⁸ The use of xenogeneic materials for restorative surgery can also present ethical and religious complexities that can be imposing.^{3,9} Research into bioceramic composites is playing an increasingly important role in the repair, reconstruction, and replacement of hard tissues. The use of synthetic materials for tissue repair or replacement is generally unencumbered by the ethical and religious concerns associated with the use of xenogeneic materials. Although synthetic materials lessen the threat of certain forms of rejection, challenges to the development of biomaterials that exhibit desirable chemical, physical, and mechanical properties remain daunting. The morphologies of the desired materials are often quite complex, and even if the desired structures can be constructed, the biological and biomechanical viability is not certain a priori.

* To whom correspondence should be addressed. E-mail: jredepen@unl.edu.
† University of Nebraska, Lincoln.

‡ Present address: Department of Chemistry, Newman University, Wichita, KS 67213.

§ Present address: Department of Chemistry, University of Wisconsin, Madison, WI 53706.

|| University of Nebraska Medical Center.

(1) (a) Guthrie, D. *A History of Medicine*; J. B. Lippincott: Philadelphia, 1949; pp 7–9. (b) Westbroek, P.; Marin, F. *Nature* **1998**, 392, 861.

(2) Bobbio, A. *Bull. Hist. Dent.* **1972**, 20, 1.

(3) Albar, M. A. *The Fountain* **1995**, 12–34.

(4) Owens, B. D.; Kragh, J. F.; Macaitis, J.; Svoboda, S. J.; Wenke, J. C. *J. Orthop. Trauma* **2007**, 21, 254.

(5) Ratner, B. D. *Biomaterials Science: An Introduction to Materials in Medicine*; Elsevier: Boston, 2004.

(6) Stock, U. A.; Vacanti, J. P. *Ann. Rev. Med.* **2001**, 52, 443.

(7) Townsend, C. M.; Beauchamp, R. D.; Evers, B. M.; Mattox, K. L. Section IV. Transplantation and Immunology. In *Sabiston Textbook of Surgery*, 17th ed.; Saunders: Philadelphia, 2004.

(8) Bach, F. H. *Annu. Rev. Med.* **1998**, 49, 301.

(9) Albar, M. A. *Saudi J. Kidney Dis. Transplant* **1996**, 7, 109.

Emerging strategies for bone repair and replacement are focused on materials that are biomimetic and often bioinspired.^{10–15} Described below is an environmentally benign and straightforward procedure for constructing composites of poly-L-lactide (PLLA)^{16,17} and hydroxyapatite (HA) that exhibit macroscopic morphologies and mechanical properties similar to those of mammalian cortical bone. We anticipate that this process may lead to straightforward methods of preparing biomimetic materials for bone fixation and repair.

Experimental Section

X-ray powder diffraction was performed using a Rigaku D-Max/B Horizontal Q/2Q X-Ray diffractometer. The resulting diffraction patterns were referenced to standards from the International Centre for Diffraction Data. ¹H NMR spectra were obtained in CDCl₃ using 400 and 500 MHz Bruker DRX Avance spectrometers. All chemical shifts (δ) are reported in ppm referenced to the solvent peak, which was assigned a value of 7.26 ppm. Molecular weights were estimated using a Viscotek VE 2001 GPC and are referenced to polystyrene standards (Viscotek). All such determinations used tetrahydrofuran (Fisher, HPLC grade) as the mobile phase and a Viscotek VE 3580 refractive index detector. Scanning electron microscopy (SEM) was performed using a Hitachi S4700 Field-Emission microscope. Hydroxyapatite surface areas were determined using the Brunauer, Emmett, and Teller (BET) method and a Micromeritics ASAP 2010 Analyzer. Mechanical properties of the composites were measured using a single-axis Instron model 1123 electromechanical machine. Prior to being tested, samples were machined into rods that were nominally 1.2 cm in length and 0.6 cm in diameter. The specimens were then subjected to compression testing using a 1.0 mm/min crosshead speed.

L-Lactide (Purac) was purified by sublimation and then stored under a nitrogen atmosphere for later use. Water was purified by reverse osmosis (General Electric E4) and then ion exchange (Barnstead NANOpure) to a specific resistance of $\geq 17.3\text{M}\Omega\cdot\text{cm}$.

Hydroxyapatite was prepared following a method first developed by Tiselius.¹⁸ For example, a 0.1 M basic solution was prepared by dissolving 48.0 g of NaOH pellets (Fisher, 97+%) in 12 L of H₂O. To this solution, 60.0 g of CaHPO₄·2H₂O (Aldrich, 98%) was added. The resulting reaction mixture was refluxed for 72 h with stirring. At the end of this time, the reaction mixture was cooled to room temperature, filtered through 5 μm filter paper, washed multiple times with water, and then dried under vacuum at 80 °C for 24 h.

Rods of anorganic bone were prepared as follows.¹⁹ Cylindrical bone plugs were machined in the longitudinal direction from the diaphyseal section of bovine femurs (Premium Protein Products) using a 6 mm diameter dowel tool. The bone plugs were then

extracted repeatedly for at least 48 h using a Soxhlet extractor containing an 80/20 (v/v) mixture of 1,2-diaminoethane (Sigma, 99%) and water. At the end of this time the plugs were repeatedly extracted with water for 4 h. The water was then replaced, and the extractions were continued for an additional period of 24 h. Extracted samples were dried in air at 75 °C, heated at 600 °C in air for at least 8 h, and then cooled under vacuum before being stored under nitrogen gas for later use. Anorganic bone was also prepared using embalmed human bone tissue that was loaned by the Anatomical Board of Nebraska. These samples were embalmed using a "Woodburn solution," which was comprised of an aqueous solution containing 33% (by volume) isopropanol, 8% glycerin, 2% formalin, and 6.7% phenol.²⁰

Composites of anorganic bone and poly-L-lactide (PLLA) were prepared by placing a section of anorganic bone (vide supra) in a Pyrex tube with excess L-lactide, all of which were stored under nitrogen gas. The tube was then cooled in liquid nitrogen and sealed at reduced pressure ($<100\text{ }\mu\text{Torr}$). The reaction vessel was then heated in a convection oven at 130 °C, typically for 7 to 10 days. The amount of L-lactide used for each reaction was dependent on the dimensions of the reaction vessel, but sufficient L-lactide to completely immerse the sample was always used. Generally speaking, a minimum of approximately 2 g of L-lactide was required for each gram of the rod derived from anorganic bovine bone (vide supra). At the end of the selected reaction time, excess monomer was allowed to drain from the sample while being maintained near 130 °C. The sample was then allowed to cool to room temperature, and any residual monomer was removed mechanically or by solvent extraction with ethanol.

All kinetics reactions were performed under nitrogen in Pyrex tubes, the closures for which were Teflon caps containing an O-ring seal. Once loaded with desired quantities of synthetic hydroxyapatite and L-lactide, the sealed reaction vessels were placed in an oil bath at a predetermined temperature between 115 and 160 °C. The oil bath was enclosed in a convection oven that was set to the same predetermined temperature, and the contents of the reaction vessel were mechanically stirred at a rate that was sufficient to guarantee that the reaction was not limited by mass transfer. Aliquots of the reaction mixture were periodically removed from the reaction vessel through a threaded access port that was normally sealed with a screw. These aliquots were removed under a stream of nitrogen gas and thermally quenched prior to being characterized using ¹H NMR to determine the extent of polymerization.

Results and Discussion

The procedure we describe below uses the nucleophilic surface of HA to initiate ring-opening polymerization of L-lactide to PLLA in the absence of any additional catalyst or solvent. The polymerization is initiated simply by heating the monomer above its melting point in the presence of HA. The resulting HA/PLLA melt can be molded and then machined using conventional technology or it can be cast directly into the desired shape (see Supporting Information). We also find that these composites can be prepared using natural sources of HA such as anorganic bone, which is the fragile inorganic structure that remains after the organic constituents have been removed from bone tissue.¹⁹ These organic components are the primary cause of undesirable immune responses.⁸ Shown in Figure 1 is a composite prepared by polymerizing L-lactide within the pores of

- (10) Roy, D. M.; Linnehan, S. K. *Nature* **1974**, 247, 220.
- (11) Westbroek, P.; Marin, F. *Nature* **1998**, 392, 861.
- (12) Petite, H.; Viateau, V.; Bensaïd, W.; Meunier, A.; de Pollak, C.; Bourguignon, M.; Oudina, K.; Sedel, L.; Guillemin, G. *Nat. Biotechnol.* **2000**, 18, 959.
- (13) Mayer, G. *Science* **2005**, 310, 1144.
- (14) Sanchez, C.; Arribart, H.; Guille, M. M. G. *Nat. Mater.* **2005**, 4, 277.
- (15) Dragnea, B. *Nat. Mater.* **2008**, 7, 102.
- (16) Middleton, J. C.; Tipton, A. J. *Biomaterials* **2000**, 21, 2335.
- (17) Kaihara, S.; Matsumura, S.; Mikos, A. G.; Fisher, J. P. *Nat. Protocols* **2007**, 2, 2767.
- (18) Tiselius, A.; Hjerten, S.; Levin, O. *Arch. Biochem. Biophys.* **1956**, 65, 132.
- (19) ASTM F1581-99: Standard Specification for Composition of Anorganic Bone for Surgical Implants. In *Book of Standards*; American Society for the Testing of Materials: West Conshohocken, PA, 2007; Vol. 13.01.

- (20) Woodburne, R. T.; Lawrence, C. A. *Anat. Rec.* **1952**, 114, 507.



Figure 1. Diaphyseal section of human femur that was converted to anorganic bone and subsequently reconstituted with poly-L-lactide.

anorganic bone derived from human cortical bone. For this particular sample the anorganic bone was heated in the presence of L-lactide at 130 °C, a temperature higher than the melting point of the monomer. Upon melting, the L-lactide rapidly infused the porous framework of the anorganic bone where its polymerization was initiated at the HA surface. The reaction was continued until the nascent polymer phase blocked mass transfer of monomer to propagation sites embedded within interstitial regions previously occupied by the organic constituents of the living bone. It is evident that the macroscopic morphology of both the compact cortical and the porous cancellous structures of the original tissue is largely conserved.

Scanning electron microscopy (SEM) reveals that the microscopic morphology of the original bone tissue is also highly conserved in composites prepared using this method. Figure 2a is an SEM image of a cryofractured HA/PLLA composite prepared from a section of anorganic bone derived from a porcine femur. For comparative purposes we show in Figure 2b a sample of anorganic porcine cortical bone that has not been reacted with L-lactide. This figure provides a broader and more representative context for the specific features visible in reconstituted sample shown in Figure 2a. The oblique cross-section in Figure 2a shows the lamellar structure that is typical for cortical bone in the diaphyseal region of mammalian long bones. The Haversian canals, the ca. 50 μm diameter structures that run the length of the osteon and serve as the primary structural unit of mature bone, are filled with PLLA. In transverse cross sections of osteons, these canals are nominally cylindrical but appear to be elliptical in this sample due to the oblique angle at which the fracture happened to occur. Also apparent are smaller, partially filled lacunae, the cavities that formerly housed individual osteocytes within the living bone.

The apparent integrity of the interface between the HA (bright areas) and the PLLA (dark areas) in Figure 2a is significant. We observe no preferential fracturing at HA/PLLA interfaces in any of the SEM images we acquired for our composites, whether they are composites of particulate synthetic HA and PLLA or anorganic bone infused with PLLA. Given the difference in coefficients of thermal expansion of the bulk materials, one might anticipate fractures at the interface between the HA and the PLLA during the cryofracturing process. If the interactions between the organic and the inorganic were weak, the preferred direction of fracture would be in the plane of the HA/PLLA interface, where the shear forces are greatest during the cryofracturing process.

Fourier transform infrared spectroscopy (FTIR) suggests the presence of strong electrostatic interactions between the HA and the PLLA phases of composites prepared using HA as the initiator. It appears that there is a bidentate interaction between the carboxylate end group of the polymer and surface-bound calcium ions. Infrared spectra of pulverized HA/PLLA composites (see Supporting Information) exhibit bands at approximately 1600 and 1315 cm^{-1} that are consistent with those observed by Qiu *et al.* for hydroxyapatite samples that have been derivatized with lactate bound to the surface through a bidentate interaction.²¹ These same bands are also quite intense in the IR spectrum for pure calcium lactate.

Compressive stress-strain curves for anorganic cortical bone reconstituted with PLLA reveal mechanical properties that can meet or exceed the original properties of the bone. We found the ultimate compressive strength of 10 reconstructed samples of cortical bone obtained from bovine femurs to be $194 \pm 26 \text{ MPa} = \bar{x} \pm 1s$. Compressive failure of the samples occurred via the typical brittle failure mechanism described by Renshaw and Schulson²² (see Supporting Information). The elastic modulus of the same set of samples was found to be $8.85 \pm 0.5 \text{ GPa} = \bar{x} \pm 1s$, and the molecular weight was $7.5 \pm 1.5 \text{ kD} = \bar{x} \pm 1s$. Tables containing the raw data for these characterizations are found in the Supporting Information. The extent to which we can manipulate the molecular weight to control mechanical properties remains unclear, but it seems likely that both the molecular weight and the polydispersity of the resulting polymer is determined by the volume distribution of interstices within the anorganic bone. For comparative purposes, we note that Yamada reports the ultimate compressive strength of the cortical bone from wet bovine femurs to be 144 MPa and the elastic modulus to be 8.52 GPa.²³ The compressive strength of human femurs is known to peak at 167 MPa for persons from 20 to 29 years of age, but it gradually declines to approximately 140 MPa for persons from 60 to 69 years of age.²³ It is also noteworthy that Verheyen *et al.* reported the compressive strength and elastic modulus for high molecular weight PLLA to be ap-

(21) Qiu, X.; Hong, Z.; Hu, J.; Chen, L.; Chen, X.; Jing, X. *Biomacromolecules* **2005**, *6*, 1193.

(22) Renshaw, C. E.; Schulson, E. M. *Nature* **2001**, *412*, 897.

(23) Yamada, H. *Mechanical Properties of Locomotor Organs and Tissues. In Strength of Biomaterials*; Evans, F. G., Ed.; William Wilkins Co.: Baltimore, 1970.

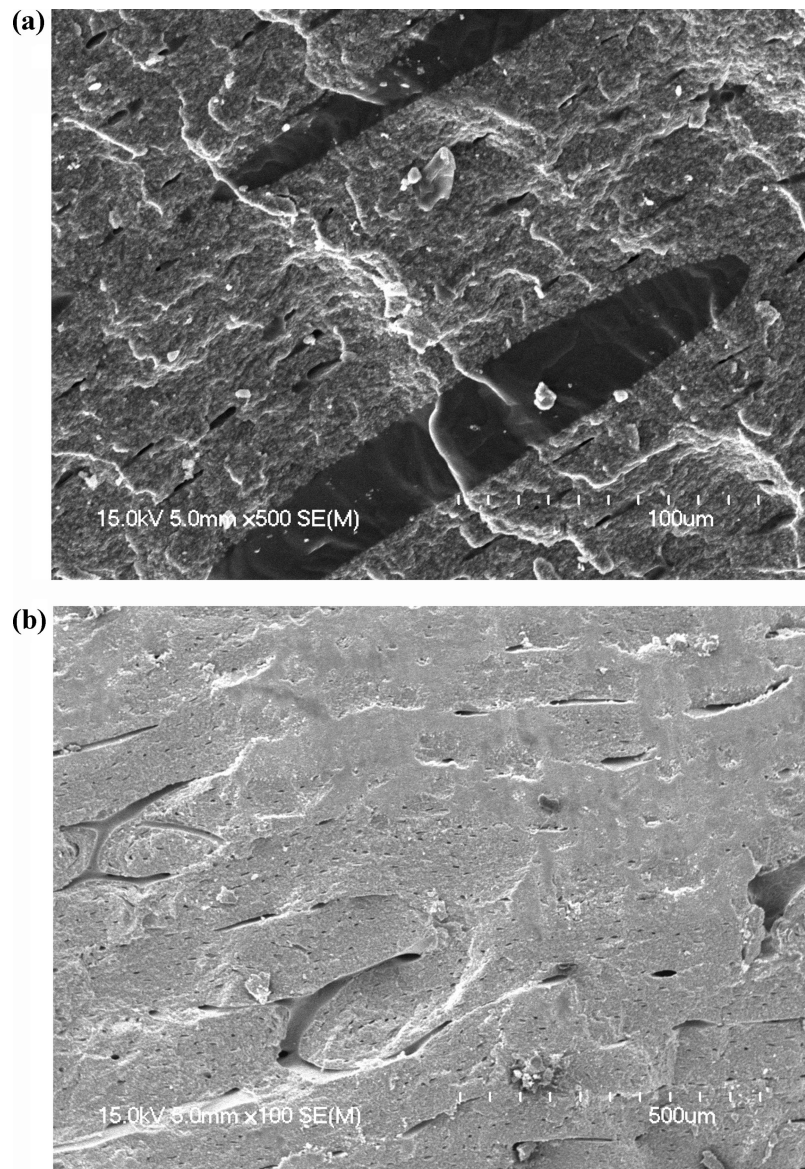


Figure 2. (a) SEM image of cryofractured composite of anorganic cortical bone (porcine) and poly-L-lactide. (b) SEM image of cryofractured anorganic cortical bone (porcine) prior to being reacted with L-lactide.

proximately 125 MPa and 5.3 GPa, respectively; however, these authors also found that if L-lactide is polymerized with stannous octoate in the presence of HA particles, the compressive, torsional, and flexural strengths decrease as the percent HA increases.²⁴

Figure 3 shows results of a series of experiments designed to characterize the kinetics of the ring-opening polymerization of L-lactide using synthetic hydroxyapatite. For the kinetics experiments shown in Figure 3, different mass ratios of HA to L-lactide were heated together in a sealed tube at 132 °C. The total mass of the reaction mixture for each of these experiments was generally from 2 to 3 g, and the mixtures were stirred to ensure that convective mass transfer was not rate limiting. Aliquots of the reaction mixture were removed and thermally quenched at regular intervals. ¹H NMR spectra such as the one shown in the inset to Figure 3 were used to quantify the relative amounts of monomer and polymer at selected times during polymerization. As can be seen from the assignments provided in Figure 4 for L-lactide and PLLA, the multiplet centered in the NMR spectrum at a chemical shift of approximately 5.16

ppm is due to methine protons in isotactic poly-L-lactide. The quartet at approximately 5.04 ppm is associated with the methine protons in nonreacted L-lactide monomer. By comparing the integrated intensities of these multiplets, one can directly compare the relative amounts of monomer and polymer in a reaction mixture as a function of time. In Figure 3, $-\log(X_t/X_0)$ is plotted versus time, where $X_0 = 1$ and is the mole fraction of monomer at time $t = 0$. X_t is the mole fraction of monomer at times $t > 0$. The zero intercept and the linear time dependence of $-\log(X_t/X_0)$ is consistent with a first-order kinetic equation

$$-\frac{dX_t}{dt} = k_{app}X_t \quad (1)$$

where the integrated form of the rate expression is

$$-\ln\frac{X_t}{X_0} = k_{app}t \quad \text{or} \quad k_{app} = -2.303\frac{\log X_t}{t} \quad (2)$$

These results provide some general insights into the mechanism by which polymerization occurs. In order for the first-order kinetic model to fit, there must be no induction period

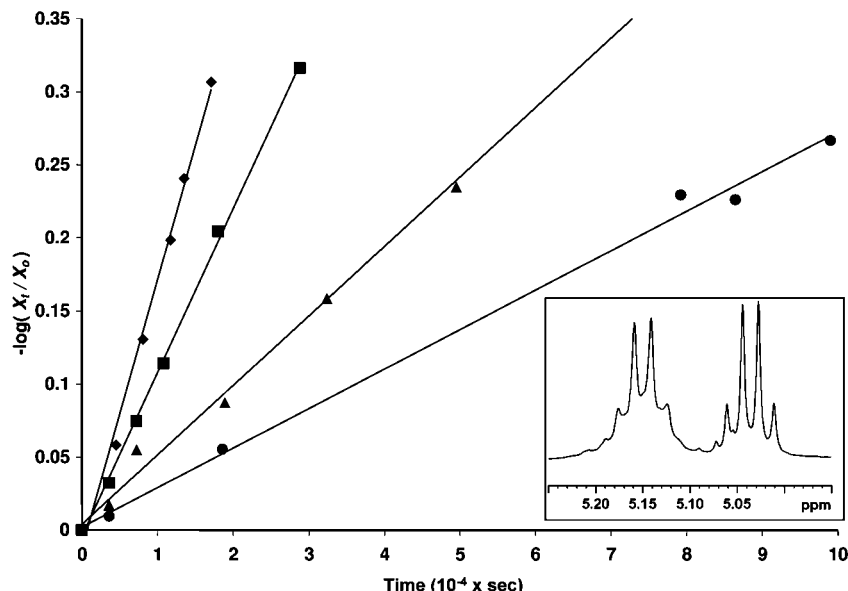


Figure 3. Kinetics for the melt polymerization of L-lactide by hydroxyapatite where the following mass ratios of L-lactide to HA were used: (◆) 2.00, $k_{app} = (4.0 \pm 0.1) \times 10^{-5} \text{ m}^{-2} \text{ s}^{-1}$; (▲) 4.00, $k_{app} = (2.58 \pm 0.05) \times 10^{-5} \text{ m}^{-2} \text{ s}^{-1}$; (■) 8.00, $k_{app} = (1.10 \pm 0.02) \times 10^{-5} \text{ m}^{-2} \text{ s}^{-1}$; (●) 16.0, $k_{app} = (6.3 \pm 0.2) \times 10^{-6} \text{ m}^{-2} \text{ s}^{-1}$. The specific surface area of hydroxyapatite for these experiments was $59.1 \text{ m}^2 \text{ g}^{-1}$.

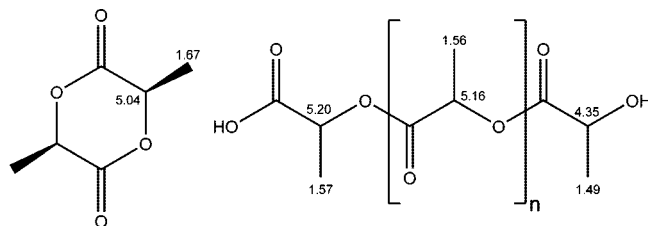


Figure 4. Chemical structures and NMR chemical shift assignments for L-lactide and poly-L-lactide.

before the HA initiator becomes active. Any induction period involving slow steps prior to chain initiation would manifest itself as a nonzero intercept in plots of $\log(X/X_0)$ vs time. Moreover, the linearity of the plots indicates that the number of initiating sites plus chain propagating sites remains constant during the course of the reaction. The k_{app} in eqs 1 and 2 is a pseudo-first-order rate constant that depends on the surface area of the hydroxyapatite initiator used per unit mass of monomer (A_S), a constant quantity that does not appear explicitly in the above expressions. The surface area determines the original number of sites that initiate polymerization and, thus, the number of sites available for chain propagation. If we model the relationship between the apparent first-order rate constant and A_S by $k_{app} = kA_S^x$, where k is the heterogeneous rate constant, then a plot of $\log k_{app}$ vs $\log A_S$ should be linear. The slope of the resulting line provides the order of the reaction as it relates to A_S , and the intercept provides $\log k$. A linear response does result when the values of k_{app} for the reactions shown in Figure 3 are plotted versus surface area (see Supporting Information). At the 90% confidence level the slope of this line is 0.91 ± 0.20 , a result that is consistent with the reaction being first order in surface area of hydroxyapatite per gram of L-lactide. The intercept of this plot gives a value of $(2.3 \pm 0.4) \times 10^{-6} \text{ g}^1 \text{ m}^{-2} \text{ s}^{-1}$ for k . Although the small value of k dictates

the use of a much larger amount of initiator than is usually used for coordination-insertion catalysts,^{25–33} this small rate constant is not a significant detriment to the reaction rate because up to two-thirds by weight of the desired composites can be hydroxyapatite.

To determine the activation energy for the surface-initiated polymerization of L-lactide by hydroxyapatite, we measured the temperature dependence of k_{app} . More specifically, ^1H NMR was used to measure $-\log(X/X_0)$ as a function of time at a series of different temperatures. The well-known Arrhenius equation (eq 3),

$$k_{app} = A e^{-E_{act}/RT} \quad (3)$$

where E_{act} is the activation energy, R is the ideal gas constant, and A is the pre-exponential factor, was used to interpret the dependence of k_{app} on temperature. Figure 5 shows the time dependence of k_{app} over a temperature range from 115 to 160 °C when the mass ratio of L-lactide to hydroxyapatite was set to 2. In other words, given that the hydroxyapatite used for these experiments had a specific surface area of

- (25) Chamberlain, B. M.; Cheng, M.; Moore, D. R.; Ovitt, T. M.; Lobkovsky, E. B.; Coates, G. W. *J. Am. Chem. Soc.* **2001**, *123*, 3229.
- (26) Chisholm, M. H.; Galucci, J.; Krempner, C.; Wiggenhorn, C. *Dalton Trans.* **2006**, *6*, 846.
- (27) Chisholm, M. H.; Galucci, J. C.; Phomphrai, K. *Inorg. Chem.* **2004**, *43*, 6717.
- (28) Kim, J.-B.; Huang, W.; Wang, C.; Bruening, M.; Baker, G. L. *Bottle Brush Brushes: Ring-Opening Polymerization of Lactide from Poly(hydroxyethyl methacrylate) Surfaces*. In *Polymer Brushes: Synthesis, Characterization, Applications*; Advincula, R. C., Brittain, W. J., Caster, K. C., Ruhe, J., Eds.; Wiley-VCH: New York, 2004; pp 105–117.
- (29) Kricheldorf, H. R.; Kreisersanders, I.; Boettcher, C. *Polymer* **1995**, *36*, 1253.
- (30) O'Keefe, B. J.; Hillmyer, M. A.; Tolman, W. B. *J. Chem. Soc., Dalton Trans.* **2001**, *15*, 2215.
- (31) Schuetz, S. A.; Silvernail, C. M.; Incarvito, C. D.; Rheingold, A. L.; Clark, J. L.; Day, V. W.; Belot, J. B. *Inorg. Chem.* **2004**, *43*, 6203.
- (32) Witzke, D. R.; Narayan, R.; Kolstad, J. J. *Macromolecules* **1997**, *30*, 7075.
- (33) Zhang, L. F.; Shen, Z. Q.; Yu, C. P.; Fan, L. *Polym. Int.* **2004**, *53*, 1013.

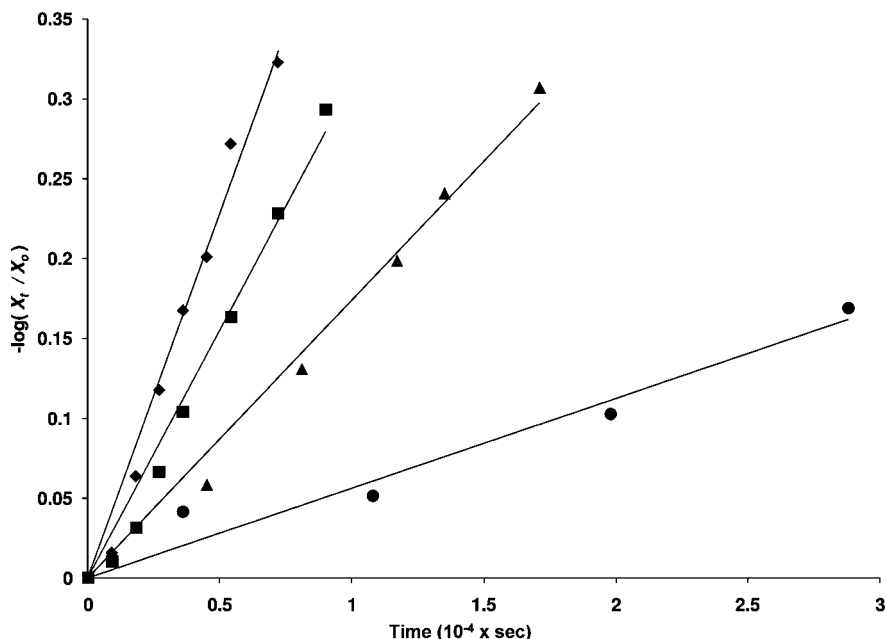


Figure 5. First-order kinetic fits at four different temperatures. The mass ratio of L-lactide to hydroxyapatite was fixed at 2:1 for each of these reactions: (●) 115 °C, $k_{app,115} = (1.3 \pm 0.1) \times 10^{-5} \text{ m}^{-2} \text{ s}^{-1}$; (▲) 132 °C, $k_{app,132} = (4.0 \pm 0.1) \times 10^{-5} \text{ m}^{-2} \text{ s}^{-1}$; (■) 147 °C, $k_{app,147} = (7.1 \pm 0.3) \times 10^{-5} \text{ m}^{-2} \text{ s}^{-1}$; (◆) 160 °C, $k_{app,160} = (1.05 \pm 0.04) \times 10^{-5} \text{ m}^{-2} \text{ s}^{-1}$.

59.1 m²/g, for each of the plots shown in Figure 5 the surface area of hydroxyapatite was 29.6 m² per gram of L-lactide. A plot of $\log k_{app}$ vs $1/T$, calculated from the slopes shown in Figure 5, is linear, and the slope of the resulting line gives an activation energy of $65 \pm 7 \text{ kJ/mol}$. This value is comparable to at least two examples in which polymerization of L-lactide is catalyzed via a coordination-insertion mechanism involving acyl-oxygen cleavage and subsequent chain propagation steps. Witzke et al. determined the activation energy for the melt polymerization of L-lactide with Sn(octanoate)₂ to be 70.9 kJ/mol.³² More recently, Zhang et al. found the activation energy to be 69.6 kJ/mol for polymerization of D,L-lactide with a La³⁺ aryloxide, which is also believed to function through a coordination-insertion mechanism similar to that of Sn(octanoate)₂.³³

Our characterizations of the polymerization process are consistent with observations by Cerrai et al.³⁴ and Guerra et al.,³⁵ who investigated the utility of hydroxyapatite in polymerizing ϵ -caprolactone, with observations by Helwig et al., who examined the utility of stannous octoate in polymerizing a series of cyclic lactones in the presence of HA,³⁶ and with experimental results of Sugiyama et al., who used sintered hydroxyapatite to initiate the polymerization of L-lactide.³⁷ Although the details of the reaction mechanism remain obscure, our results indicate that polymerization of L-lactide by HA is initiated by surface nucleophiles, probably hydroxide ions^{38,39} or strongly bound water, to cleave the

acyl-oxygen bond in L-lactide. Samples of solid Ca₃PO₄ and CaSO₄ do not initiate polymerization of L-lactide under conditions similar to those that are effective when HA is used as the initiator. The negative results for these controls are expected given that neither phosphate nor sulfate are considered to be strong nucleophiles. These controls also indicate that calcium ions alone do not serve as an effective initiator for polymerization of L-lactide. Rapid polymerization of L-lactide was observed for separate sets of controls using CaO and Ca(OH)₂ as the heterogeneous initiator; however, it is presently unclear if the initiation step for these compounds, which could involve proton extraction from the lactide ring, is similar to that for hydroxyapatite. Our qualitative results using CaO and Ca(OH)₂ are consistent with earlier results by Kricheldorf and Serra, who showed that CaO and MgO initiate polymerization of L-lactide with significant racemization associated with an initial proton abstraction step.⁴⁰ We do not, however, observe significant racemization for HA-initiated polymerization of L-lactide.

Although our efforts to use the nucleophilic surface of anorganic bone to prepare biomimetic composites with PLLA are still in their infancy, the composites presently exhibit mechanical properties that are quite similar to those of living bone. Future investigations will more thoroughly map out reaction conditions that are efficacious in producing desirable composites of anorganic bone with PLLA and other cyclic lactones including poly-D,L-lactide, poly glycolide, poly- ϵ -caprolactone, and copolymers of these monomers. Additional mechanical assessments are certainly needed, including tensile, bending, and torsional characterizations. Such measurements will be done in conjunction with *in vivo* resorption studies to evaluate the biological performance of our composites. The overall goal of these research efforts will be to investigate the extent to which resorption properties

(34) Cerrai, P.; Guerra, G. D.; Tricoli, M.; Krajewski, A.; Guicciardi, S.; Ravaglioli, A.; Maltinti, S.; Masetti, G. *J. Mater. Sci. Mat. Med.* **1999**, *10*, 283–289.

(35) Guerra, G. D.; Cerrai, P.; Tricoli, M.; Krajewski, A.; Ravaglioli, A.; Mazzocchi, M.; Barbani, N. *J. Mater. Sci. Mat. Med.* **2006**, *17*, 69.

(36) Helwig, E.; Sandner, B.; Gopp, U.; Vogt, F.; Wartewig, S.; Henning, S. *Biomaterials* **2001**, *22*, 2695.

(37) Sugiyama, N.; Kunibu, R.; Yoshizawa-Fujita, M.; Takeoka, Y.; Aizawa, M.; Rikukawa, M. *Chem. Lett.* **2007**, *36*, 1476.

(38) Cho, G.; Wu, Y.; Ackerman, J. L. *Science* **2003**, *300*, 1123.

(39) Kay, M. I.; Young, R. A. *Nature* **1964**, *204*, 1050.

(40) Kricheldorf, H. R.; Serra, A. *Polym. Bull.* **1985**, *14*, 497.

and mechanical performance can be fine tuned to meet expectations dictated by the design criteria for specific orthopedic devices for bone fixation and restoration.

Acknowledgment. The University of Nebraska Research Council supported this research. The UCARE program at the University of Nebraska—Lincoln provided a fellowship for

J.D.S. Discussions with Dennis Chakkalakal are a pleasure to acknowledge.

Supporting Information Available: FTIR spectra, X-ray powder diffraction, kinetic data, mechanical characterizations, and photographs (PDF). This material is available free of charge via the Internet at <http://pubs.acs.org>.

CM800895R